Volume 13
Number 15
21 April 2022
Pages 4183–4426

Chemical Science

rsc.li/chemical-science

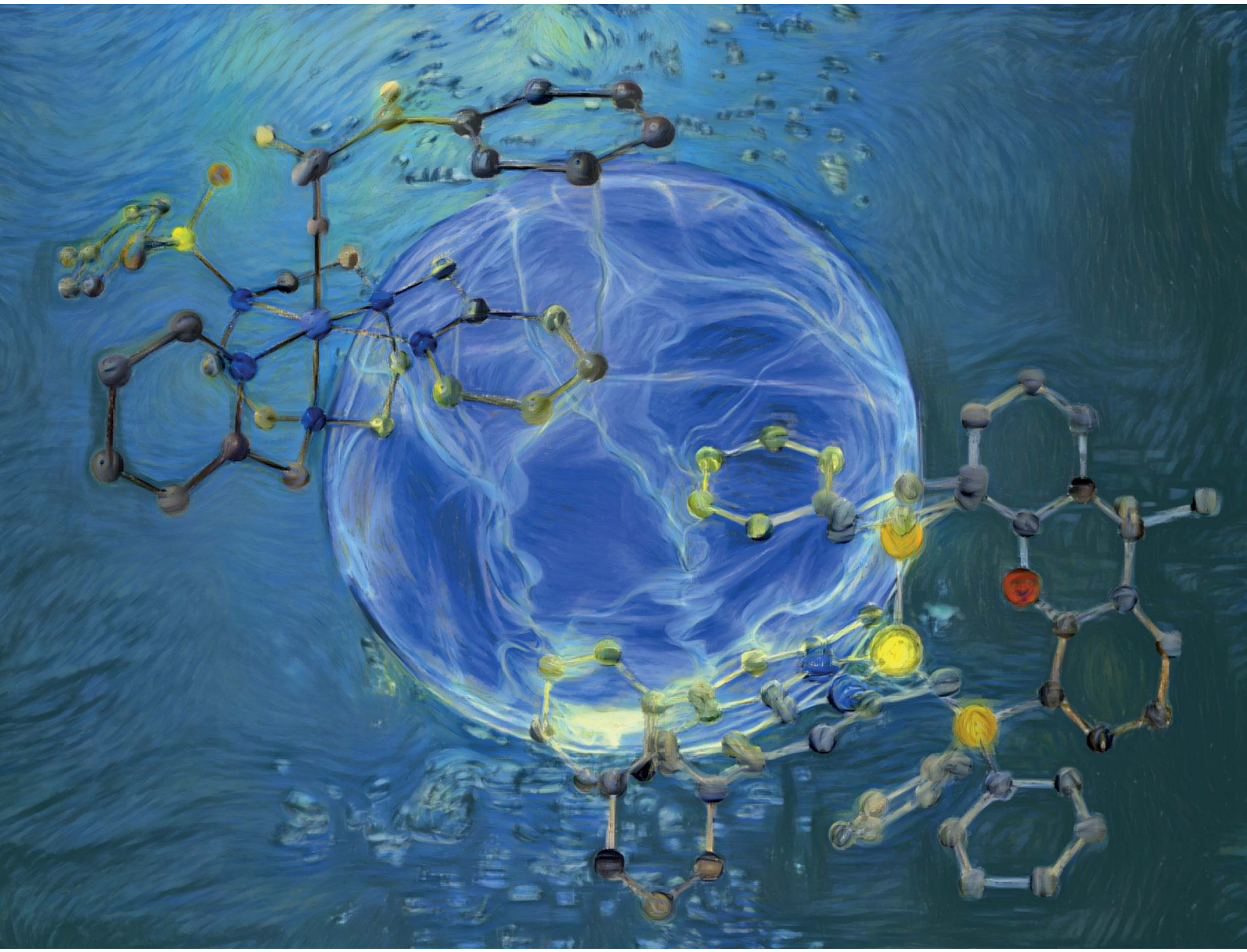

ISSN 2041-6539

ROYAL SOCIETY OF CHEMISTRY

EDGE ARTICLE

Julio Lloret-Fillol *et al.*

Light-driven reduction of aromatic olefins in aqueous media catalysed by aminopyridine cobalt complexes

Chemical Science

ROYAL SOCIETY OF CHEMISTRY

EDGE ARTICLE

View Article Online
View Journal | View Issue

Cite this: *Chem. Sci.*, 2022, **13**, 4270

All publication charges for this article have been paid for by the Royal Society of Chemistry

Light-driven reduction of aromatic olefins in aqueous media catalysed by aminopyridine cobalt complexes†

Carla Casadevall, [a] David Pascual,[a] Jordi Aragón,[a] Arnau Call, [a] Alicia Casitas,[a] Irene Casademont-Reig [b] and Julio Lloret-Fillol *[ac]

Received 26th November 2021
Accepted 9th March 2022

DOI: 10.1039/d1sc06608k

rsc.li/chemical-science

A catalytic system based on earth-abundant elements that efficiently hydrogenates aryl olefins using visible light as the driving-force and H_2O as the sole hydrogen atom source is reported. The catalytic system involves a robust and well-defined aminopyridine cobalt complex and a heteroleptic Cu photoredox catalyst. The system shows the reduction of styrene in aqueous media with a remarkable selectivity (>20 000) *versus* water reduction (WR). Reactivity and mechanistic studies support the formation of a [Co–H] intermediate, which reacts with the olefin *via* a hydrogen atom transfer (HAT). Synthetically useful deuterium-labelled compounds can be straightforwardly obtained by replacing H_2O with D_2O. Moreover, the dual photocatalytic system and the photocatalytic conditions can be rationally designed to tune the selectivity for aryl olefin *vs.* aryl ketone reduction; not only by changing the structural and electronic properties of the cobalt catalysts, but also by modifying the reduction properties of the photoredox catalyst.

Introduction

The use of sunlight as driving force is a promising but challenging strategy towards sustainability in chemical production.[1–4] Artificial photosynthesis (AP), as a technology to provide a clean source of reductive equivalents,[4–8] has been mainly studied in the context of H_2O[9–13] and CO_2 (ref. 14–18) reduction, with still limited progress towards organic transformations.[1,2,4,8,19–32] A challenging transformation in the context of AP is the hydrogenation of double bonds.[8] Among difficulties, most developed protocols employing the activation of H_2, silanes or alcohols are not suitable for operation under aqueous conditions.[33–37] And only a few studies used light as a driving force and most of them have been carried out in the absence of water as a solvent. Moreover, selectivity of olefin reduction *versus* water reduction is needed for achieving a practical use in the context of AP. In the case of aromatic olefins, they are prompted to form radicals, tending to polymerize under such conditions.[38]

In the context of AP, semiconductor materials such as TiO_2 and CdS were initially used as catalysts for the light-driven hydrogenation of electron-deficient olefins. These systems required UV light (λ = 365 nm) and noble metals to obtain moderate selectivity for alkane formation (Scheme 1a).[39–41] Another remarkable example employed a B_{12}–TiO_2 hybrid for the UV light-driven reduction of alkenes to alkanes.[42] Such highly energetic conditions led to the formation of dimeric products compromising the selectivity.[43]

Holland, Corma and co-workers introduced the stereoselective hydrogenation of the conjugated C=C bond of ketoisophorone by combining the photocatalytic activity of Au nanoparticles supported on TiO_2 with the enzymatic activity of oxidoreductases by means of FAD^+ as a mediator and cofactor (Scheme 1b).[22] Likewise, Hartwig, Zhao and co-workers reported a cooperative chemoenzymatic reaction that combines the isomerization of C=C by an iridium photoredox catalyst with the hydrogenation activity of ene-reductases to selectively reduce electron-deficient aromatic olefins to their corresponding alkanes in high enantiomeric excess (88–99% ee).[44] All of these previous studies show that light-driven reduction of alkenes is feasible, albeit limited in substrate scope, selectivity and yield.

Very recently, X. C. Cambeiro and co-workers reported the use of an iridium photosensitizer in combination with a Hantzsch ester for the reduction of aromatic 1,2-disubstituted alkenes, albeit good yields were obtained only for activated olefins.[45] At the same time, M. Kojima, S. Matsunaga and co-workers found that glyoxime type complexes with a PCy_3 ligand

[a]*Institute of Chemical Research of Catalonia (ICIQ), The Barcelona Institute of Science and Technology, Avinguda Països Catalans 16, 43007 Tarragona, Spain. E-mail: jlloret@iciq.es*

[b]*Donostia International Physics Center (DIPC), Polimero eta Material Aurreratuak: Fisika, Kimika eta Teknologia, Kimika Fakultatea, Euskal Herriko Unibertsitatea UPV/EHU, P.K. 1072, 20080 Donostia, Euskadi, Spain*

[c]*Catalan Institution for Research and Advanced Studies (ICREA), Passeig Lluïs Companys, 23, 08010, Barcelona, Spain*

† Electronic supplementary information (ESI) available. See DOI: 10.1039/d1sc06608k

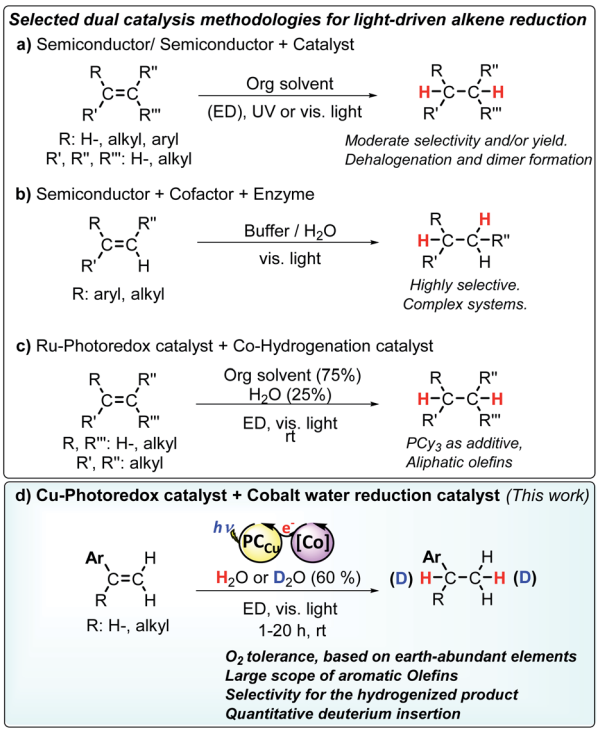

Scheme 1 Selected dual catalysis methodologies for the light driven reduction of olefins. Abbreviations: ED: electron donor. Selected references: (a) ref. 8 and 10, (b) ref. 11, (c) ref. 12 and (d) the developed methodology in this study.

and a ruthenium photoredox catalyst reduce aliphatic alkenes *via* a hydrogen atom transfer (HAT) mechanism.[46] However, aromatic alkenes have additional difficulties such as their tendency to engage in radical polymerization[38] or isomerization reactions[47–49] under reductive conditions, which makes their reduction under photocatalytic conditions more challenging (Scheme 1). By a conceptually different approach, X. Guo, O. S. Wenger and co-workers recently reported the reduction of olefins by the photo-HAT reactivity of the organometallic iridium hydride complex [Cp*Ir^{III}(phen)–H] in acetonitrile.[50] Polyzos and co-workers showed the reduction of aromatic olefins *via* direct photoinduced electron transfer under highly reductive conditions and light intensity.[51]

Ideally, AP systems should employ water as a source of hydrogen atoms and efficiently use the photoredox catalyst in combination with molecular catalysts to facilitate the selective reduction of alkenes. Such an approach should identify catalysts' hits to develop more complex AP schemes. Towards this goal, we previously reported a dual catalytic system formed by [Co(OTf)(Py$_2^{Ts}$tacn)](OTf) (**1**) (Py$_2^{Ts}$tacn = 1,4-di(picolyl)-7-(*p*-toluenesulfonyl)-1,4,7-triazacyclononane, OTf = trifluoromethanesulfonate anion) as a reduction catalyst and [Cu(bathocuproine)(xantphos)][PF$_6$)[52] (**PC$_{Cu}$**) as a photoredox catalyst, which efficiently reduces water to hydrogen[53] and carbonyl groups to alcohols, using water as a hydrogen source.[29] Our mechanistic studies suggested that a cobalt(II) hydride ([Co(H)(Py$_2^{Ts}$tacn)]$^+$, [Co^{II}–H]) was a common intermediate in both reduction reactions. Based on these precedents, we

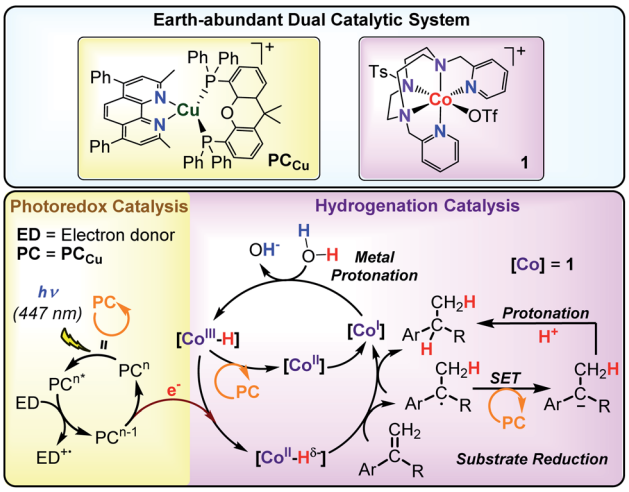

Scheme 2 Earth-abundant dual catalytic system for the photoreduction of aromatic olefins.

hypothesized that [Co(H)(Py$_2^{Ts}$tacn)]$^+$ should also be reactive enough to engage in the reduction of other organic functionalities without the need for strong reducing agents.[31]

Herein, we present a dual catalytic system consisting of cobalt complexes based on nitrogenated ligands (**1–15**), different Ir and Cu photoredox catalysts and an electron donor for the reduction of styrene derivatives using light as an energy source. The reduction operates without the use of typical reducing agents such as silanes, H_2, HCO_2H or alcohols. The best performing catalytic system is obtained by combining [Co(OTf)(Py$_2^{Ts}$tacn)](OTf) (**1**) and **PC$_{Cu}$** under light irradiation employing H_2O/Et_3N as a hydride source (Scheme 2).[29–32] This synthetic methodology also allows for replacing H_2O by D_2O to produce the analogous deuterated alkanes. Reactivity and mechanistic studies based on kinetics, isotopic labelling and radical clock experiments suggest that the reduction of aromatic olefins occurs *via* a HAT mechanism, most likely through a [Co–H] intermediate. According to our mechanistic findings, the interplay between the catalyst/substrate redox potential, together with the light intensity, provides a way to control the selectivity for the reduction of aromatic olefins *versus* aromatic ketones and *vice versa*. This unique behaviour is rationalized by the different reduction mechanisms that each substrate undergoes.

Results and discussion

Based on previous studies,[29,30] we hypothesized that the putative [Co(H)(Py$_2^{Ts}$tacn)]$^+$ intermediate formed under photochemical conditions may engage in the reduction of more challenging substrates, such as styrene (**16**). The irradiation ($\lambda = 447 \pm 20$ nm ; $T = 35$ °C) of a solution containing styrene (**16**, 16.5 mM), complex **1** (1 mol%) as a reduction catalyst, **PC$_{Cu}$** (1.5 mol%) as a photoredox catalyst, and Et_3N (0.2 mL, 8.5 equiv.) as a sacrificial electron donor in a H_2O : CH_3CN (6 : 4 mL) solvent mixture, produced ethylbenzene (**16a**) in good yield (67%) (Table S.8, entry 1†). The reduction of styrene is accompanied by

small amounts of styrene dimerization (butane-2,3-diyldibenzene, **16b**, 11% yield). The detection of this homocoupling product suggests the formation of benzylic radicals during the reaction, whose mechanistic implications will be discussed later (see the Mechanistic studies section).

(I) Screening of conditions and the catalytic system

The formation of homocoupling product **16b** was significantly minimized (4%) by increasing the catalyst and photoredox catalyst loadings (from 1.5 to 3 mol%) and reducing the styrene concentration (from 16.5 to 8.7 mM), yielding ethylbenzene (**16a**) in 86% yield. Further refinement of the reaction conditions was achieved by adjusting the reaction temperature. It is worth noticing that the reaction yield and selectivity are sensitive to the temperature. At 35 °C or higher, the yield of the reduced product drops in favour of the reduced homocoupling product. Therefore, the reaction temperature should be effectively controlled to prevent warming by light irradiation. Despite the common LED intensity (~2.1 W at 447 nm) used, the produced heat is enough to warm up the reactions to 45 °C if the temperature is not controlled.

We have used an in-house developed parallel photoreactor to precisely control the temperature and light intensity (see the ESI for further details†).[29,54] At 25 °C, the formation of the homocoupling product was only 3% (Table 1, entry 4) and negligible at 15 °C (Table 1, entry 5 and Table S8†). At lower temperatures, the homocoupling product was detected only in traces. We rationalized that the reduction of the selectivity at higher temperature is most likely due to accumulation of benzylic radicals, which then favour dimerization. Under optimized conditions, the hydrogenation of styrene yields **16a** in 91% yield without detection of dimeric products (Table 1, entry 5).

Control experiments determined that all components of the photocatalytic system (light, the cobalt catalyst, photoredox catalyst and electron donor) are necessary for the formation of **16a** or **16b.** In the absence of light, **1**, $\mathbf{PC_{Cu}}$, or Et_3N (Table 1, entries 6–9), neither **16a** nor **16b** was observed. To discard the formation of benzylic radicals from a direct single electron transfer (SET) reduction from the reduced photoredox catalyst ([Cu(bathocuproine)(xantphos)], $\mathbf{[PC_{Cu}]^0}$) to styrene, we performed photocatalytic studies in the absence of complex **1**. Even when the reaction was performed at 55 °C using 32 mM **16** and 10 mol% $\mathbf{PC_{Cu}}$, no dimeric products were observed, discarding direct SET from $\mathbf{[PC_{Cu}]^0}$ to styrene (Table S.9†). Indeed, $\mathbf{[PC_{Cu}]^0}$ is not reductive enough to transfer an electron to **16** ($E(\mathbf{PC_{Cu}}^{I/0})$ = −1.60 and E_{red} = −2.31 V *vs.* SCE for **16**). Additionally, no reduced products were detected when **1** was replaced by cobalt salts such as the starting cobalt(II) triflate ($Co(OTf)_2(MeCN)_2$, Table 1 entry 10). We found practically that the reduction yield of **16** was equivalent when complex **1** was synthesized *in situ* by adding the Py_2^{Ts}tacn ligand with an equimolar amount of $Co(OTf)_2(MeCN)_2$ (Table 1 entry 11) under catalytic conditions.

The effect of the photoredox catalyst. On the other hand, replacement of the photoredox catalyst $\mathbf{PC_{Cu}}$ by [Cu(bathocuproine-I)(Xantphos)](PF_6) ($\mathbf{^{I}PC_{Cu}}$) or [Cu(bathocuproine-SO_3^-)(xantphos)](Na) ($\mathbf{^{SO3}PC_{Cu}}$) produced **16a** in lower yield (21 and 78%, respectively). We also tested three different iridium photosensitizers with different substituents on the bipyridine

Table 1 Optimization of the catalytic conditions for the reduction of **16** using PC_{Cu} as a photoredox catalyst and **1** as a catalyst[a]

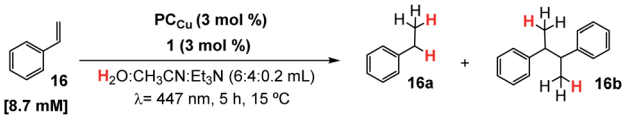

Entry	Deviation from conditions	% **16a**	% **16b**
1	16.5 mM **16**, 35 °C, **1** (1 mol%), and $\mathbf{PC_{Cu}}$ (1.5 mol%)	67	11
2	16.5 mM **16** and 35 °C	81	6
3	35 °C	86	4
4	25 °C	90	3
5	None	91	n.d.
6	No light	n.d.	n.d.
7	No Et_3N	n.d.	n.d.
8	No $\mathbf{PC_{Cu}}$	n.d.	n.d.
9	No **1**	n.d.	n.d.
10	$Co(OTf)_2(MeCN)_2$ instead of **1**	n.d.	n.d.
11	[$Co(OTf)_2(MeCN)_2$ + Py_2^{Ts}tacn] instead of **1**	91	n.d.
12	$\mathbf{^{I}PC_{Cu}}$ instead of $\mathbf{PC_{Cu}}$	21	n.d.
13	$\mathbf{^{SO3}PC_{Cu}}$ instead of $\mathbf{PC_{Cu}}$	78	n.d.
14	$\mathbf{^{H}PC_{Ir}}$ instead of $\mathbf{PC_{Cu}}$	11	8
15	$\mathbf{^{NMe2}PC_{Ir}}$ instead of $\mathbf{PC_{Cu}}$	67	n.d.
16	$\mathbf{^{CO2H}PC_{Ir}}$ instead of $\mathbf{PC_{Cu}}$	47	8
17	$\mathbf{1_{Ni}}$ instead of **1**	n.d.	n.d.

[a] Conditions: **1** (mol%), **PC** (mol%), and **16** (mM) as indicated in the table in H_2O : CH_3CN : Et_3N (6 : 4 : 0.2 mL), irradiation at λ = 447 nm for 5 h at 35, 25 or 15 °C under N_2. Yields were determined by GC analysis after workup of the reaction and relative to a calibrated internal standard. Values are average of triplicates. [Ni(OTf)(Py_2^{Ts}tacn)](OTf) ($\mathbf{1_{Ni}}$). See the ESI for the synthesis and characterization of metal complexes.

that tuned their redox potential: $[Ir(ppy)_2(bpy)](PF_6)$ ($^{H}PC_{Ir}$), $[Ir(ppy)_2(dcbpy)](PF_6)$ ($^{CO2H}PC_{Ir}$) and $[Ir(ppy)_2(dmab)](PF_6)$ ($^{NMe2}PC_{Ir}$) (Table 1 entries 12–16 and Fig. S.26 and S.27†). Although the yields showed only a weak correlation with the PC redox potentials, in general, higher product yields are obtained with the more reducing photoredox catalysts ($^{CO2H}PC_{Ir}$, $^{H}PC_{Ir}$, $^{I}PC_{Cu}$, PC_{Cu}, $^{SO3}PC_{Cu}$, $^{NMe2}PC_{Ir}$, $E^{I/0} = -1.01$, -1.40, -1.47, -1.60, -1.66, and -1.80 V *vs.* SCE yielded 47, 11, 21, 91, 78, and 67% yield of **16a**, respectively), suggesting an interplay between the photochemical properties of the photocatalysts, cobalt catalysts and substrates. For instance, there is a change in selectivity for the most reducing ^{NMe2}**PCIr**, since the yield of **16a** decreased due to the formation of other subproducts, which could be interpreted as a faster formation of benzylic radical intermediates. On the other hand, in the absence of a catalyst, we observed negligible styrene reduction.

The effect of the cobalt complex. Then, we explored the capacity of other cobalt complexes as catalysts, including tetra- and pentadentate aminopyridine cobalt complexes that are active for the photochemical ketone reduction,[29] as well as commercially available cobaloxime and vitamin B_{12} to reduce **16** under the established standard photocatalytic conditions (Table 2). Interestingly, the photocatalytic activity varies depending on the nature of the complex.

Although a correlation between molecular properties of the cobalt complex and reaction yield is not straightforward, we noticed that complexes with the tacn ligand scaffold are among the best catalysts. For instance, the lowest yield was obtained by complex **7**, which has also the lowest reduction potential in Table 2, whereas the highest yield was obtained by complex **1** ($E^{II/I} = -0.97$ and -1.15 V *vs.* SCE, respectively, Fig. S.26†). Finally, replacing the cobalt centre by nickel in complexes **1**, **2** and **6** did not yield any reduced product.

Selectivity for 16a *versus* 16b. Selectivity towards olefin reduction *versus* a homocoupling product ($Sel_{16a/16b}$ calculated as n(**16a**)/n(**16b**)) varies depending on the cobalt complex. Among the series tested, complex **1** was the most efficient and selective catalyst for olefin reduction (91% yield **16a**, <1% yield **16b**, $Sel_{16a/16b} = 91$). The results evidenced that the tacn ligand scaffold (**1** and **9–14**) provides the best yield and an excellent selectivity for the reduction of **16** (yield 76 to 91%, $Sel_{16a/16b} =$ 91–11, Table 2 and Fig. S.29†). Catalysts **2–7** (aminopolypyridyl ligands) yielded a maximum of 47% for **16a**, together with a loss in selectivity ($Sel_{16a/16b} =$ 24–2.6%). Cobaloxime ([Co^{III}(Cl)(Py)(Glioxime)], **8**) achieved **16a** in 51% yield but with a significantly higher amount of **16b** as a by-product (25% yield, $Sel_{16a/16b} = 2$). Whereas vitamin B_{12} was the less active and selective catalyst of the series, yielding only traces of both reduced and dimeric products (4 and 6% yield, respectively, $Sel_{16a/16b} = 0.7\%$).

Selectivity for 16a *versus* H_2. The hydrogen evolution reaction is usually an overlooked reaction in studies involving photoreduction of organic substrates, but it is an essential feature for further progress in photocatalyzed reduction of organic substrates in water involving reduced metal complexes. It is well-known that aminopyridine cobalt complexes are efficient catalysts for hydrogen evolution under similar photocatalytic conditions (Fig. S.30 and S.31†).[29,30,53,55]

Co complexes with aminopyridyl-tacn derived ligands [$Co^{II}(OTf)_2(^{Y,X}Py^{Me}tacn)$] (series **9–14** $^{Y,X}Py^{Me}tacn$ = 1-[(4-X-3,5-

Table 2 Photocatalytic reduction of styrene (**16**) to ethylbenzene (**16a**) by the selected WR cobalt complexes[a]

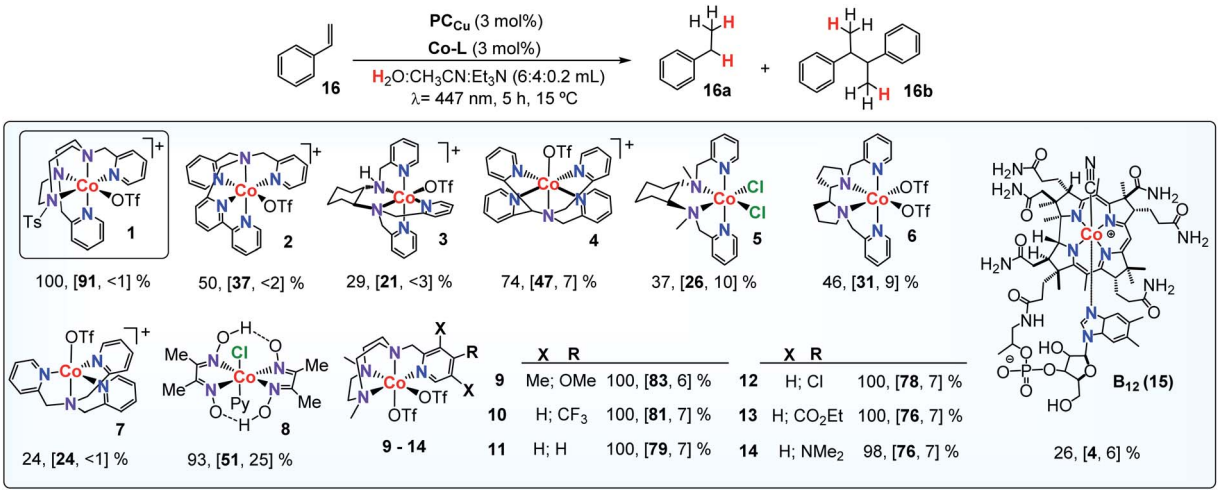

[a] Selected WR complexes: **1**: [$Co^{II}(OTf)(Py_2{}^{Ts}tacn)$](OTf), **2**:[$Co^{II}(OTf)$(DPA-Bpy)](OTf), **3**: [$Co^{II}(OTf)(N_4Py)$](OTf), **4**: [$Co^{II}(OTf)$(H-CDPy$_3$)](OTf), **5**:[$Co^{II}(OTf)_2$(PDP)], **6**: [$Co^{II}(OTf)_2$(TPA)], **7**: [$Co^{II}(Cl)_2$(BpcMe)], **8**: [Co^{III}(Cl)(Py)(Glioxim)], **9**: [$Co^{II}(OTf)_2(^{Me,OMe}Py^{Me2}tacn)$], **10**: [$Co^{II}(OTf)_2(^{H,CF3}Py^{Me2}tacn)$], **11**: [$Co^{II}(OTf)_2(^{H,H}Py^{Me2}tacn)$], **12**: [$Co^{II}(OTf)_2(^{H,Cl}Py^{Me2}tacn)$], **13**: [$Co^{II}(OTf)_2(^{H,CO2Et}Py^{Me2}tacn)$], **14**: [$Co^{II}(OTf)_2(^{H,NMe2}Py^{Me2}tacn)$] and **15**: vitamin B_{12}. Conditions A: **Co-Cat** (261 μM, 3 mol%), PC_{Cu} (261 μM, 3 mol%), and **16** (17.4 μmol, 8.7 mM) in H_2O : CH_3CN : Et_3N (6 : 4 : 0.2 mL), irradiation (447 nm) for 5 h at 15 °C under N_2. Yields were determined by GC analysis after workup relative to a calibrated internal standard. Values were average of triplicates and correspond to conversion and [**16a** and **16b** yield].

Y-2-pyridyl)methyl]-4,7-dimethyl-1,4,7-triazacyclononane) have been reported among the fastest catalysts for H_2 production with TOF, TON, and quantum efficiencies as high as 52 000 h^{-1}, 9000, and 9.7% ± 1.0 for complex **13**.[55] In this regard, the photocatalytic reduction of **16** was accompanied by the formation of H_2 as a side-product, in analogy to ketone and aldehyde reduction reactivity.[29] The formation of H_2 during the styrene reduction was monitored using pressure sensors[29,56] and quantified by analysis of the reaction headspace using Gas Chromatography-thermal conductivity detector (GC-TCD, see the ESI for further details†). As expected, the selectivity of the studied Co complexes for the substrate *vs.* water reduction ($Sel_{16a/H2}$ calculated as n(**16a**)/n(H_2)) strongly depends on the ligand scaffold. Under optimized conditions, complex **1** is also the most active catalyst for H_2 evolution with a $Sel_{16a/H2}$ of 1.04 (Table 3 and Fig. S.30†). Nonetheless, considering the concentrations of water and **16** in catalysis (ratio H_2O/**16** ~ 19 100), the normalized selectivity for the olefin reduction is about 20 000. Reducing the water in the reaction decreased the formation of H_2 at the expense of diminishing the TON of olefin reduction.

The produced H_2 was lower for the non-tacn ligand-based catalysts (**2**–**8**), providing an excellent selectivity for **16** *versus* water reduction and also the yields ($Sel_{16a/H2}$ = 5.4–9.0, Fig. S.30†). For tetradentate tacn-based complexes **9**–**14**, increasing the electron donating character of the ligand disfavours the H_2 evolution, complex **10** being the most efficient for H_2 evolution in the presence of the alkene ($Sel_{16a/H2}$ = 0.8 for **10**, Fig. S.31†).[30] The 15-fold selectivity difference between **9** and **10** (*p*-MeO- *versus* *p*-CF_3-) illustrates the ligand control in the selective olefin/water reduction.

(II) Scope of the reaction

With the optimal conditions in hand, we examined the scope of aromatic olefins.

Monosubstituted styrene derivatives. Monosubstituted styrene derivatives with either electron-withdrawing or donating groups at the arene (**16**–**27**) are reduced within 5 h with excellent yields (73–99%) (Table 3). The reduction of *p*-bromostyrene (**22**) to *p*-bromoethylbenzene (**22a**) is obtained in moderate yield (53%), attributed to the partial formation of the reduced dehalogenated product in 19% yield. This is consistent with the previously reported reduction of aryl halides giving aryl radicals by visible light-induced electron transfer processes.[57] In the case of styrenes containing chlorine and fluorine atoms at the aromatic ring (**23**–**25**), the hydrogenation occurred without dehalogenation (Table 2).[58] Interestingly, the CF_3 substituted aromatic styrene derivative (**26**) was compatible with the reaction conditions. Finally, substrate **27**, with potentially problematic pyridine coordination, yielded the reduced product with excellent yield (99%).

1,1-Disubstituted olefins. Under optimized reaction conditions, the reduction product of 1,1-disubstituted aryl-alkyl olefins (**28a**–**32a**, Table 3) was accompanied by the reductive coupling of two olefins (**28b**–**32b**, Table 3, conditions A). We

Table 3 Light-driven reduction of selected aromatic mono- and 1,1-disubstituted olefins

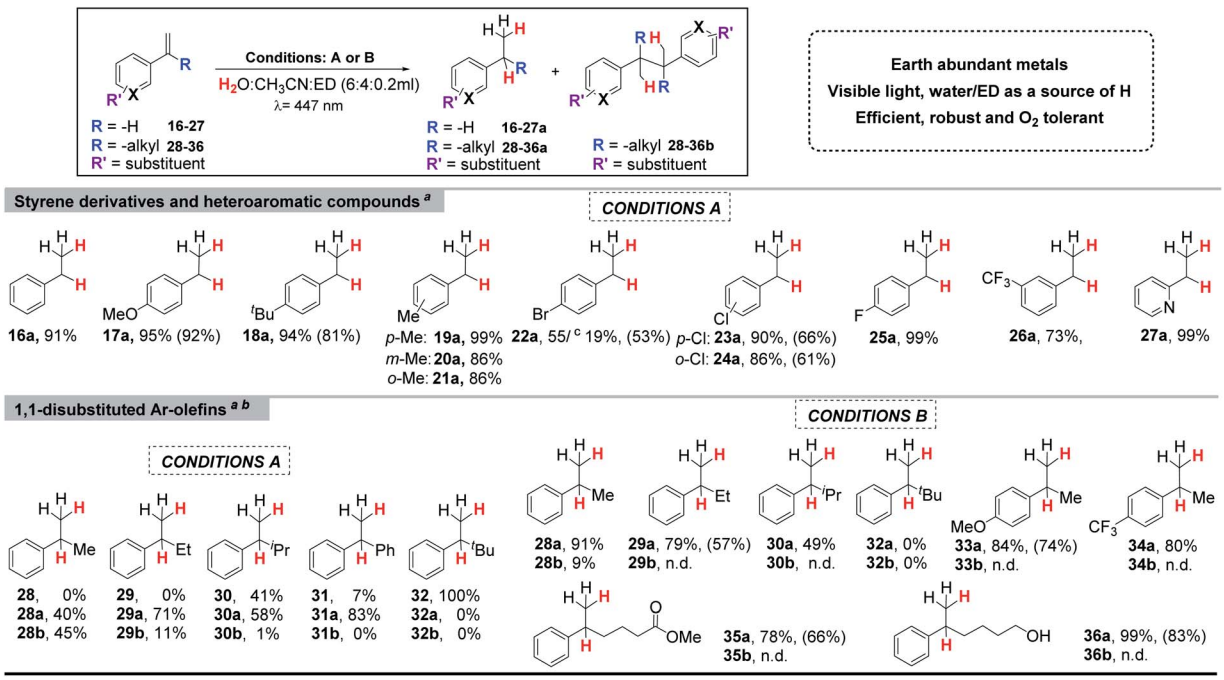

[a] Conditions A: **1** (3 mol%), PC_{Cu} (3 mol%), and the substrate (8.7 mM) in H_2O : CH_3CN : Et_3N (6 : 4 : 0.2 mL), irradiated for 5 h (447 nm) at 15 °C under N_2. [b] Conditions B: **1** (6 mol%), PC_{Cu} (6 mol%), and the substrate (4.4 mM) in H_2O : CH_3CN : $^iPr_2EtN$ (6 : 4 : 0.2 mL), irradiated for 24 h (447 nm) at −3 °C under N_2. Yields after workup (average of triplicates) were determined by GC analysis relative to a calibrated internal standard. Isolated yields between parentheses (average of 16 parallel reactions). [c] Yield of the reduced dehalogenated product.

rationalized the formation of homocoupling products as an indication of the presence of highly reactive benzylic radicals. For 1,1-disubstituted aryl-alkyl alkenes, it can be argued that these benzylic radicals are more stable against a single electron reduction surviving long enough to dimerize (see the Mechanistic studies section).

Such benzylic radicals could be formed by a HAT reaction from the [Co–H] intermediate to the less hindered carbon of the olefin, in agreement with the previously observed selectivity for M–H species.[59–61] These results are also in agreement with recent reactivity reported on the reduction and homo- and heterocoupling of alkenes using silanes as reducing agents;[62,63] and on the reactivity of putative [Co–H] species with olefins by J. Norton and co-workers,[64,65] as well as the recent studies of M Kojima, S. Matsunaga and co-workers.[46] Nevertheless, it is well-known that cobalt hydride complexes can undergo HAT to alkenes, and it was recently shown that it can be photo-induced.[35,66]

We noted that the yield of the reductive homocoupling product decreased with the alkyl substituent size at the olefin (from –Me to ^{i}Pr), suggesting that the steric effect of the substituent influences the product selectivity, as expected for radical couplings. Moreover, the conversion of the –Me and –Et substituted alkenes (**28**and **29**) was quantitative, but not for the one with the ^{i}Pr group (**30**). With the aim to give an explanation for the lack of reactivity, we calculated and compared first the redox potentials of the olefins. As expected, the one electron reduction potential of the studied olefins is very negative (see Fig. S.26 and S.48†). However, the reaction yields are excellent for *para*-substituted arenes with a methoxide **17** and a *tert*-butyl group **18**, despite having $E_{1/2}^{0/-I}$ redox potentials of −2.50 and −2.45 V *vs.* SCE, respectively. These redox potentials are more negative than that calculated for the 1,1′-disubstituted Ph, ^{i}Pr alkenes (**30**) (−2.40 V, V *vs.* SCE), suggesting that the lower reactivity for **30** could be related to steric effects. Indeed, for the bulkier ^{t}Bu-substituted aryl-alkyl olefin (**32**), there was no conversion. This agrees with the HAT mechanism since it is very sensitive to steric effects.[67]

On the other hand, the catalytic system is inefficient towards the reduction of 1,2-disubstituted styrene derivatives (**37–41**), yielding the *trans–cis* isomerization reaction as previously reported,[47–49] and only a trace amount of the reduced product was observed (Table S.16†). This is an indication of a triplet energy transfer from $\mathbf{PC_{Cu}}$ to the disubstituted alkene. Moreover, the isomerization also occurs without the presence of the Co(II) complex **1**. However, we can reasonably propose that the energy transfer (ET) path is minor to olefins because the reductive quenching of $\mathbf{PC_{Cu}}$ considering the concentrations is 10-fold larger by Et_3N than by our model olefin **16**. Moreover, when increasing the amount of Et_3N added to the reaction, the reduction of **16** was also accelerated. If the ET mechanism was the productive path for the reduction of **16**, an increase in the Et_3N concentration should have decreased the production rate of the reduced product; however, the opposite effect was observed (Fig. S.36†).

It is worth noting that in the absence of the cobalt catalyst, neither olefin reduction nor homocoupling products were detected for the 1,1-disubstituted alkenes studied (**28–31**, Table S.15†). These results agree with the low redox potentials of **28–31** (E_{red} −2.36, −2.37, −2.40 and −2.29 V *vs.* SCE, respectively, Fig. S.26 and S.48†), that are ≥690 mV more negative than the $\mathbf{[PC_{Cu}]^0}$ reduction redox potential ($E(\mathbf{PC_{Cu}}^{I/0}) = -1.60$ V *vs.* SCE). This supports that for the studied olefins, the generation of benzylic radicals by single electron transfer (SET) from $\mathbf{[PC_{Cu}]^0}$ is not feasible.

At this point, we hypothesized that the selectivity towards olefin reduction could be improved by decreasing the temperature of the reaction. Such a decrease should have an impact on the rate of formation of [Co–H] species and then the following formation of benzylic radical species. Preventing the radical accumulation, thus, avoids the formation of homocoupling products since the reaction is second order with respect to the concentration of radicals (eqn (1) and (2), where v_{rad} and k_{rad} are the rate and the formation rate constant of the benzylic radical, respectively; [R] and [PC$^-$] are the concentration of the substrate and reduced photoredox catalyst, and v_{dim} and k_{dim} are the rate and the formation rate constant of the dimeric product, respectively). Consequently, at higher temperatures (>35 °C), the yield of the reduced product drops in favour of the homocoupling product. In addition, small quantities of trimers or higher order coupling products can be also detected by GC-MS, indicating a higher formation of radicals. In contrast, at low temperatures (15 to −3 °C, as specified per case), the dimeric products are negligible (Fig. S.32†).

$$v_{rad} = k_{rad}[R] \times [PC^{n-1}] \quad (1)$$

$$v_{dim} = k_{dim}[R]^2 \quad (2)$$

Further optimization showed that a bulkier electron donor such as diisopropylethylamine (DIPEA) favours the selectivity towards the reduced product (Tables S.8†), since it avoids formation of by-products between the electron donor and the substrate due to steric hindrance.[68] In addition, a finer tuning of the concentration of the substrate, catalyst **1** and photoredox catalyst $\mathbf{PC_{Cu}}$ (Tables S.11 to S.13†) allowed establishing optimal reaction conditions. Thus, by increasing the loading of **1** and $\mathbf{PC_{Cu}}$ (6 mol%), reducing the substrate concentration (4.4 mM), and using DIPEA at −3 °C, we achieved excellent selectivity for the reduction of 1,1-disubstituted aromatic alkenes (Table S.13† entry 5 and Table 1 conditions B).

O_2 tolerance. It is worth noticing that the photocatalytic system maintains its activity even when having O_2 in the headspace. The reduction of **16** and **28** is accomplished in 91 and 81% yields, respectively, when the reaction is carried out in air and using non-degassed solvents (Table S.17†). We rationalize these results using the capacity of the catalytic system to reduce O_2 to H_2O before reducing the olefins as we observed previously for the reduction of ketones.[29,53,69] This contrasts with the high sensitivity of organometallic complexes to O_2 when preforming hydrogenation reactions.[33,70–72]

Deuteration of olefins. Since H_2O is the source of hydrogen atoms in the developed method, we also explored the possibility to obtain deuterated products by using D_2O as a solvent. Thus,

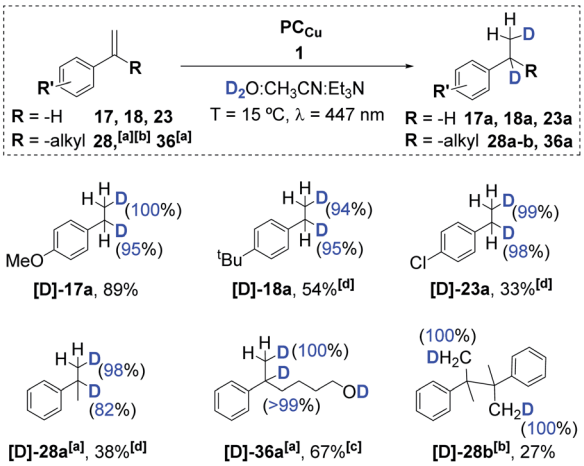

Scheme 3 Deuterium labelling studies of aromatic olefins (**17**, **18**, **23**, **28** and **36**). Conditions: **1** (3 mol%), $\mathbf{PC_{Cu}}$ (3 mol%), the substrate (8.7 mM) in H_2O : CH_3CN : Et_3N (6 : 4 : 0.2 mL) irradiated for 5 h (447 nm) at 15 °C under N_2. [a] Conditions: **1** (6 mol%), $\mathbf{PC_{Cu}}$ (6 mol%), and the substrate (4.4 mM) in D_2O : CH_3CN : $^iPr_2EtN$ (6 : 4 : 0.2 mL), irradiated (447 nm) for 24 h at −3 °C under N_2. [b] Conditions [a] modifying [Subs.] to 16 mM and 5 h at 30 °C. [c] NMR yield. [d] Low isolated yields were obtained due to the high volatility of the products. Isolated yields (average of 16 reactions). D-insertion analysed by NMR.

olefins **17**, **18**, **23**, **28** and **36** were reduced with the dual $\mathbf{PC_{Cu}}$/**1** catalytic system in a D_2O : CH_3CN mixture. We observed nearly quantitative olefin deuteration (see Fig. S.50–S.65†). Analytics showed the incorporation of one deuterium atom at each carbon atom of the double bond (α and β) (Scheme 3). Moreover, D-labelling studies of α-methylstyrene (**28**) under catalytic conditions that favour the reduced homocoupling product (high temperature and concentration of the substrate) showed the incorporation of only two deuterium atoms – each one at a different methyl group of the coupling product (Fig. S.56 and S.57†).

This agrees with the formation of M-deuteride species ([Co–D]) that are involved in a deuterium atom transfer (DAT) mechanism with the olefin, forming the corresponding benzylic radical, which dimerizes or ends up reduced and deuterated, affording the deuterated product. Moreover, we did not observe double deuteration at the same carbon nor H/D scrambling. Therefore, if organometallic cobalt species are formed after the insertion of Co–D/H in the olefin, the reversibility of the reaction *via* beta-hydride elimination should be negligible. Thus, it is more likely that benzylic radicals are directly formed *via* DAT/HAT from Co–D/H, supported by the observation of benzylic radical species. Nevertheless, an irreversible metal hydride insertion cannot be fully discarded.

(III) Mechanistic studies

To gain insight into the nature of the active species and the mechanism, we performed kinetic and reactivity studies, including D-labelling and radical clock experiments (Fig. 1).

First, kinetic studies in the presence of mercury showed that the photocatalytic activity is not inhibited, even in the presence of a large amount of mercury (>2000 eq. *vs.* **1**, Fig. 1a). This suggests that the catalysis is not related to metal (0) nanoparticles, and thus, agrees with the homogeneous nature of the active species. We also studied the influence on the reduction rate for **16** in both H_2 and N_2 atmospheres (Fig. 1b). The kinetic traces were identical regardless of the atmosphere used, indicating that the source of hydrogen in the reduced products does not come from the H_2 generated under photocatalytic conditions. Indeed, both H_2 evolution and olefin reduction are competing pathways that share a common intermediate, since with catalyst **1**, the H_2 produced decreased at higher concentrations of styrene (Fig. S.33†).

By initial reaction rate analyses, we found that both **1** and $\mathbf{PC_{Cu}}$ have a first-order reaction (Fig. 1d, S.34 and S.35†), in agreement with the bimolecular reduction mechanism of the cobalt catalyst by $\mathbf{PC_{Cu}}$. On the other hand, the reaction order found in olefin is close to zero (Fig. S.33†). Quenching studies with the copper photoredox catalyst ($\mathbf{PC_{Cu}}$) in the presence of TEA and styrene as a model substrate show similar quenching constants (K_{SV} = 94.9 M^{-1} and 109.8 M^{-1}, respectively). However, since the concentration of TEA under catalytic conditions is 10 times higher than that of styrene, we can consider the energy transfer pathway to the organic substrate to be negligible (Fig. 1e).

As introduced in the previous section, the exchange of H_2O by D_2O led to the formation of deuterated olefins with exclusive deuteration on the carbons of the olefin, and only two deuterium atoms were introduced one on each of the olefinic carbon atoms (Scheme 3 and ESI section 13† for NMR analyses). The absence of scrambling and double deuterium insertions indicates that regardless of the mechanistic path, the reaction is not reversible. On the other hand, when we employed 1,2 disubstituted olefin **41**, we did not observe deuterium insertion (Fig. S.62 and S.63†), indicating that although isomerization takes place, it is most likely to proceed through a photochemically generated exited state without the intervention of [Co–H] insertion–elimination steps.[50] As introduced above, we discard the energy transfer as a significant path responsible for the reduction of olefins since the increase of the Et_3N concentration increased the reaction rate, despite both showing a similar quenching rate of the photoredox catalyst.

Experiments with radical clocks were performed to evaluate the formation of benzyl radicals *via* a HAT mechanism as already suggested by the formation of dimeric products. Olefins containing a 2-aryl-cyclopropyl moiety at the α-position are commonly used as probes for the formation of radicals in organic transformations.[50,73] These radical clocks are very convenient because if a radical is generated in the benzylic position, it will trigger the cyclopropane ring opening with a high rate constant. For the (1-(2-phenylcyclopropyl)vinyl) benzene (**42**), cyclopropane ring opening is about 10^8 s^{-1}.[74,75] Moreover, the presence of an aromatic group at the olefin is necessary to stabilize the benzylic radical after the cyclopropane ring-opening. Without the stabilizing group, the resulting product from the cyclopropane ring-opening is endergonic and could yield wrong conclusions (Fig. S.49†).[74,75] Under catalytic

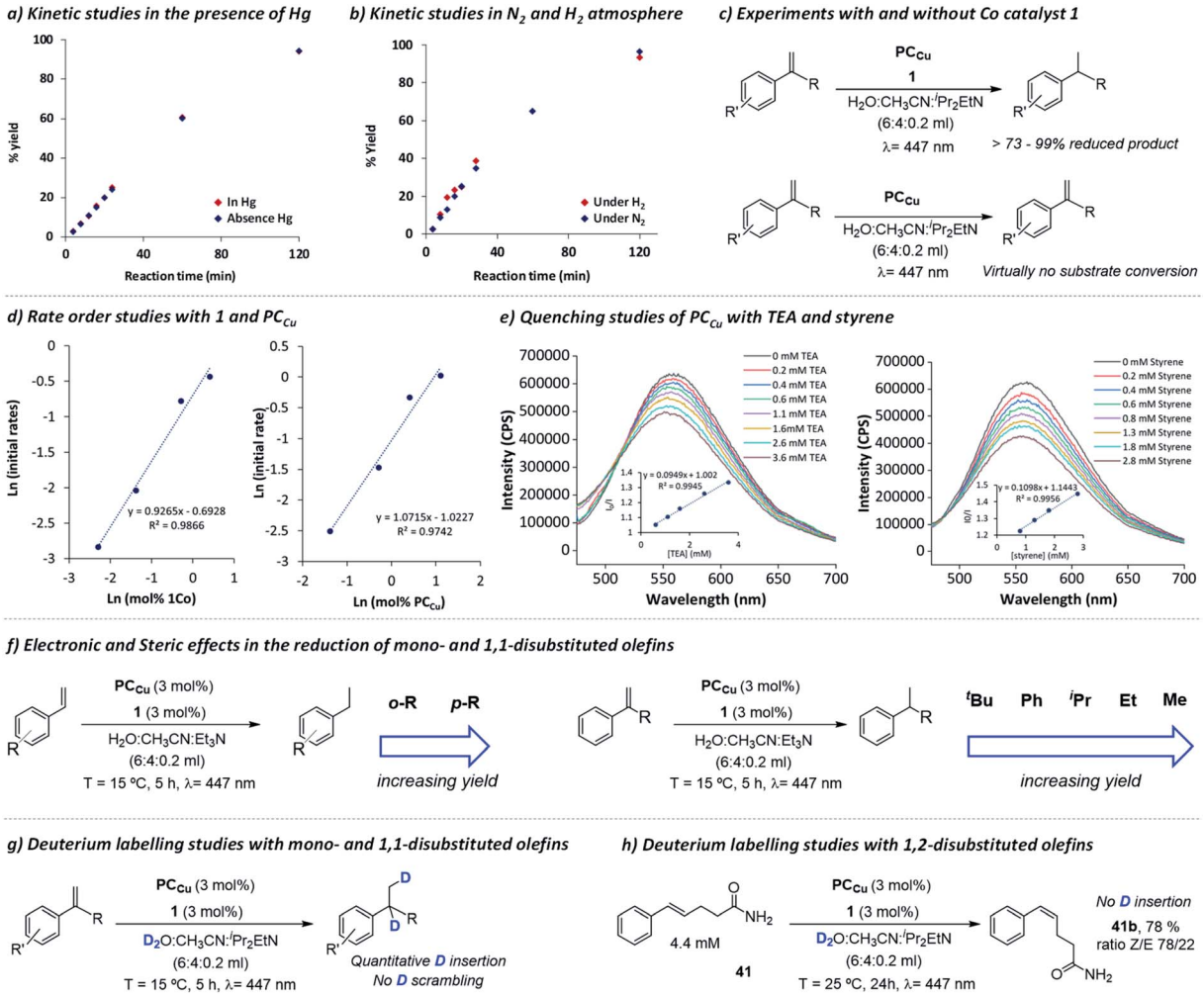

Fig. 1 Mechanistic studies. Formation of **16a** in (a) the absence (red diamonds) and presence of Hg(0) (>2000 eq.) (blue diamonds); and in (b) H_2 (red diamonds) or N_2 (blue diamonds) atmosphere. (c) Experiments with and without complex **1**. (d) Reaction rate kinetics regarding complex **1** and PC_{Cu}. (e) Reductive quenching studies of PC_{Cu} with TEA and styrene. (f) Steric effects in alkene reduction. Deuterium labelling studies of mono- and 1,1-disubstituted olefins (g) and 1,2-disubstituted olefin **41** (h, *Z*/*E* ratio analysed by NMR). See Experimental section 3 for the procedure details.†

conditions, the reduction of **42** only affords the ring-opening product (**42b**) without detection of **42a** (Scheme 4).

When the reaction was performed in D_2O, quantitative D-insertion at the β and benzylic positions was observed (**[D]-42b**, see Fig. S.64–S.70†). With the lack of the cobalt catalyst **1**, no ring-opening products were detected, fully recovering the substrate after irradiation. Both **42b** and **[D]-42b** can be formed *via* initial HAT (or DAT) from [Co–H] (or [Co–D]) followed by ring-opening and rearrangement to the most stable radical (Scheme 4).

(IV) Mechanistic discussion

Mechanisms in Scheme 5 were proposed considering the collection of experimental results. It is well-established that light irradiation (447 nm) of [Cu(bathocuproine)(xantphos)]$^+$ ($[PC_{Cu}]^+$) leads to the formation of the $^*[PC_{Cu}]^+$ excited state, which is reductively quenched in the presence of an excess of aliphatic amine (Et_3N or $^iPr_2EtN$ was used as quenchers in our study).[52] The reaction then affords the one-electron reduced $[PC_{Cu}]^0$ species ($E(PC_{Cu}{}^{I/0}) = -1.60$ V *vs.* SCE).[76,77] The reduction potentials of the studied olefins are in the range of −2.1 to −2.6 V *vs.* SCE[50] (Fig. S.48† for the theoretical values). Therefore, based on the thermodynamics of the process, the direct reduction of the studied olefins by the singly reduced species $[PC_{Cu}]^0$ could be discarded (ΔG of the reaction is endergonic by 12 to 23 kcal mol^{-1} depending on the olefin).[29]

This is supported by the lack of reduced, dimerized or ring-opening products formed when radical clock **42** ($E(42^{0/-}) = -2.36$ V *vs.* SCE) was tested in the absence of complex **1**. However, $[PC_{Cu}]^0$ is reductive enough to reduce complex **1** ($E(Co^{II/I}) = -1.15$ V *vs.* SCE) affording Co^I species.[53] We previously studied the formation of similar Co^I species under photo- and electrochemical conditions.[55,78] These low-valent intermediates can be protonated by water to form a putative [Co^{III}–H]. We previously reported that the reduction of [Co^{III}–H] to [Co^{II}–H] by $[PC_{Cu}]^0$ is largely exergonic (−17.6 kcal mol^{-1}),[29,53] and

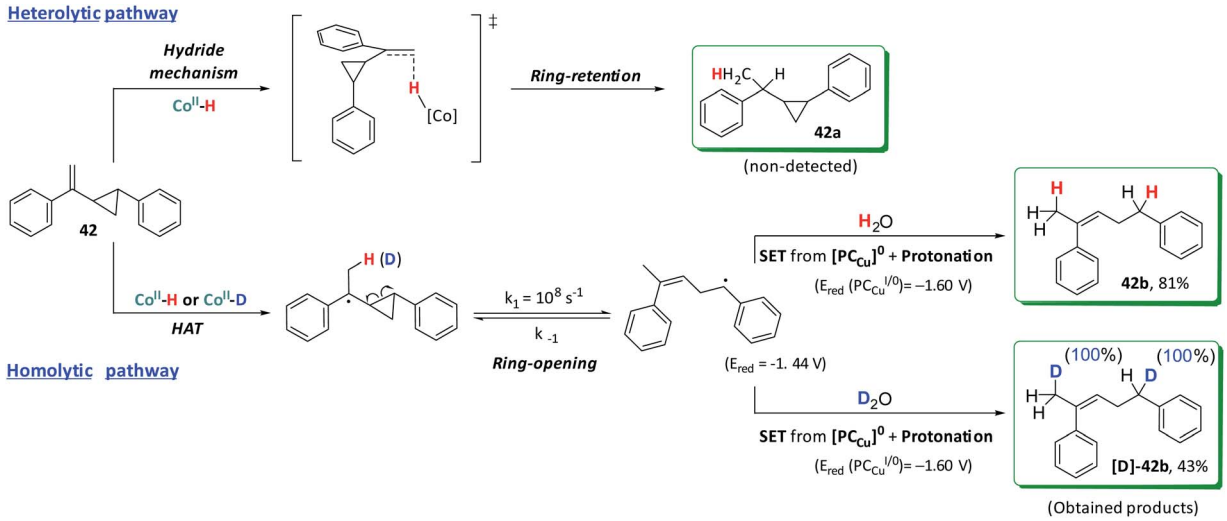

Scheme 4 Two possible reduction pathways for (1-(2-phenylcyclopropyl)vinyl)benzene (**42**).

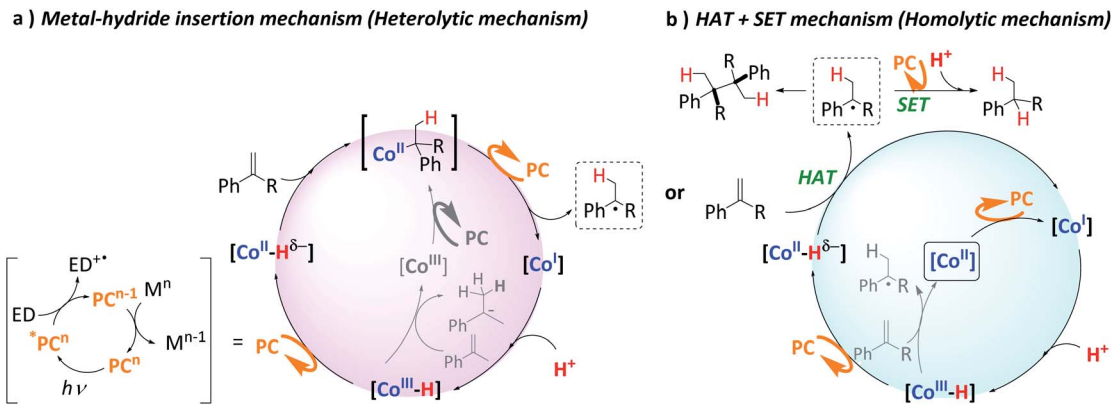

Scheme 5 Possible mechanistic scenarios for the reduction of aromatic olefins by the light-driven dual-copper–cobalt catalytic system in aqueous media. The highlighted [Co^{II}] intermediate indicates the beginning of the catalytic cycle. Acronyms stand for PC = photoredox catalyst; ED = electron donor; SET = single electron transfer and HAT = hydrogen atom transfer.

therefore, we can reasonably consider a fast ET to yield [Co^{II}–H]. Therefore, under such reducing photochemical conditions, [Co^{III}–H] should be easily converted into [Co^{II}–H] species.[29,55]

On the other hand, it is interesting that the reaction order found in the olefin is close to zero (Fig. S.33†). The fact that the reaction rate does not depend on the alkene concentration is consistent with our previous studies on hydrogen evolution and the reduction of ketones and aldehydes.[29,55] Thus, we interpreted this result as the formation of the [Co^{III}–H] complex as a rate-determining step, since the following reduction to [Co^{II}–H] species and their subsequent HAT to the olefin are fast. Moreover, as discussed above, this [Co^{III}–H] is a common intermediate for both H_2 evolution and olefin reduction.

The formation of homocoupling products and the isotopic D-labelling pattern observed, together with the radical clock experiments support that the reaction proceeds *via* the formation of benzylic radical species. As explained above, the most likely pathway to form the benzylic radicals is a HAT from [Co^{II}–H] to the β carbon of the olefin, whereas a potential metal hydride insertion is less likely, but cannot be discarded.

Although it cannot be completely ruled out, since no doubly-deuterated terminal-carbons in the reduced products were detected, this indicates that neither β-hydride elimination nor reversible HAT occurs (Scheme 5a). Then, the fastest and most likely scenario is that benzylic radicals undergo a reduction (E^{theor}_{red} = −1.44 to −1.69 V *vs.* SCE) by [PC_{Cu}]^0 (E = −1.60 V *vs.* SCE), which after subsequent protonation gives the alkane (Scheme 5b). We discard the HAT from the oxidized amine because the deuteration of the benzylic position is virtually quantitative.

(V) Mechanistically designed ketone/olefin reduction selectivity

The postulated HAT mechanism for olefin reduction (Scheme 5b) implies that the selectivity could be modulated against functional groups that are reduced *via* a different mechanism

such as SET. This is the case for our previously reported reduction of aromatic ketones using the dual catalytic system.[29]

To test our hypothesis, we used styrene (**16**) and acetophenone (**43**) as competing substrates. We previously determined, that under equivalent photocatalytic conditions, **43** is reduced to 1-phenylethanol *via* a SET mechanism from $[\mathbf{PC_{Cu}}]^{0}$ yielding the ketyl radical anion (KRA) as an intermediate ($E_{red} = -1.65$ V *vs.* SCE).[29,30] Then the generated KRA is trapped by [Co–H] to form the reduced product *via* HAT (Scheme 6). Therefore, it should be possible to differentiate the KRA formation *via* SET from the HAT mechanism of the olefin, designing rationally the photocatalytic conditions.

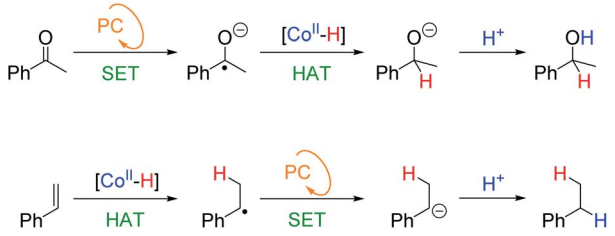

Scheme 6 Different substrate-dependent mechanisms for the observed selectivity. KRA stands for the ketyl radical anion and PC for the photoredox cycle.

This rationalization suggests that the counterintuitive idea of increasing the redox potential of the photoredox catalyst should make the catalytic system more selective. For instance, under more reducing conditions, a SET mechanism should be favoured, and therefore, the reduction of the ketone would be preferent, while the opposite would favour otherwise.

First, when similar catalytic conditions to those reported for the selective reduction of aromatic ketones *vs.* aliphatic aldehydes[29] were used (**1** (1 mol%), $\mathbf{PC_{Cu}}$ (1.5 mol%), total substrates (**16** + **43**, 16.5 mM, 1 : 1) in H_2O : CH_3CN : Et_3N (6 : 4 : 0.2 mL) irradiated for 4 h at 25 °C under N_2), acetophenone (**43**) was preferentially reduced in the presence of **16** ($Sel_{\mathbf{43a}/(\mathbf{16a}+\mathbf{43a})} =$ 65%, Fig. 2a, Table S.18 and Fig. S.37†). Then, we modified the

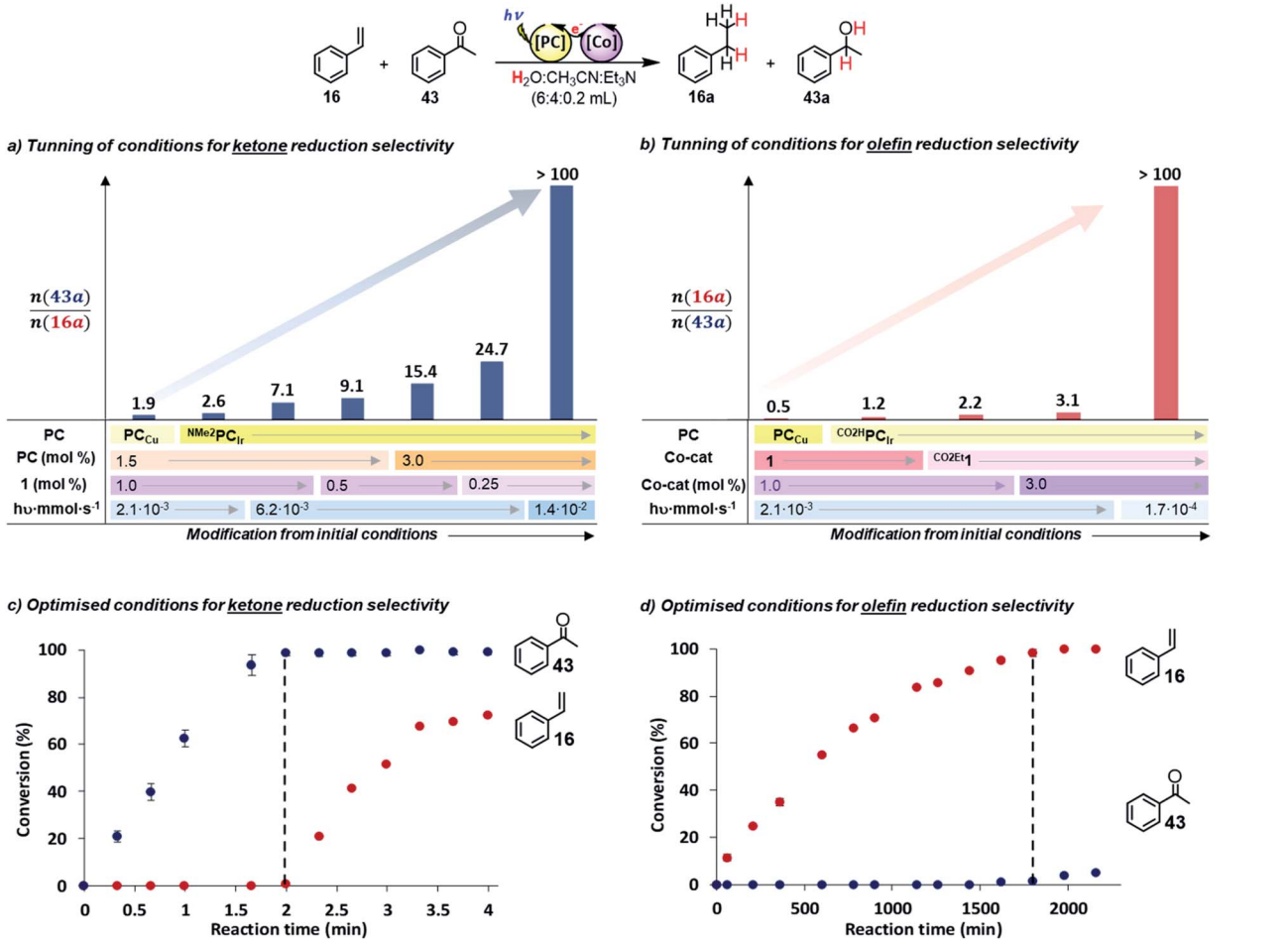

Fig. 2 Competition studies between styrene (**16**) and acetophenone (**43**). (a and b) Optimization of the photocatalytic conditions for selective reduction of **43** and **16**, respectively. Conditions: (c) **1** (0.25 mol%), $^{NMe2}\mathbf{PC_{Ir}}$ (3 mol%), total substrate concentration (**16** + **43**, 16.5 mM, 1 : 1) in a H_2O : CH_3CN : Et_3N (3 : 2 : 0.1 mL) mixture, irradiated at 447 nm (7 LED at 700 mA, 1.44×10^{-2} mmol hν s^{-1} of photons[55]) for 4 min at 25 °C under N_2. (d) $^{CO2Et}\mathbf{1}$ (3 mol%), $^{CO2H}\mathbf{PC_{Ir}}$ (1.5 mol%), total substrate concentration (16.5 mM) in a H_2O : CH_3CN : Et_3N (3 : 2 : 0.1 mL) mixture, irradiated at 447 nm (1 LED at 50 mA 1.67×10^{-4} mmol hν s^{-1} of photons[55]) for 36 h (2160 min) at 25 °C under N_2. The black dotted line indicates where substrates **16** (c) and **43** (d) start reacting.

reaction conditions to test the hypothesis of favouring either the SET to **43** or the HAT to **16**. Under stronger reducing conditions, which favour the SET initial step, we sequentially increased the reduction potential, concentration of **PC** and the light irradiation intensity. Moreover, we also decreased the concentration of complex **1** to disfavour the HAT process. To our delight, an improvement in the selectivity was observed by using $^{NMe2}\mathbf{PC_{Ir}}$ instead of $\mathbf{PC_{Cu}}$ (from 65 to 72% selectivity).

Further improvement was obtained by increasing the light intensity up to 6.2×10^{-3} mmol hν s^{-1} *vs.* the normal 2.1×10^{-3} mmol hν s^{-1},[55] which presumably increased the concentration of the reduced photoredox catalyst ($[^{NMe2}\mathbf{PC_{Ir}}]^{0}$), and thus, accelerating the SET reaction (from 72 to 88% Table S.18 and Fig. S.38 and S.39†). In contrast, the effect of complex **1** concentration was minor (from 88 to 90%). As a result, 100% selectivity for ketone **43** reduction (in 2 min) was obtained in the presence of styrene **16** using $^{NMe2}\mathbf{PC_{Ir}}$ (3 mol%, $E_{1/2}(Ir^{III/II}) = -1.80$ V *vs.* SCE), complex **1** (0.25 mol%, $E(Co^{II/I}) = -1.15$ V *vs.* SCE) and irradiation at higher light intensity (1.4×10^{-2} mmol hν s^{-1}) (Fig. 2a and c).

To favour the HAT, we modified the reaction conditions to make them less reducing. First, we used the less reductive photoredox catalyst $^{CO2H}\mathbf{PC_{Ir}}$ ($E_{1/2}(Ir^{III/II}) = -1.01$ V *vs.* SCE), and the selectivity for styrene reduction was increased by 20% (Fig. 2b, Table S.19 and Fig. S.44†). Likewise, using a less reductive Co catalyst [$(Co^{II}(OTf)(^{H,CO2Et}Py_2{}^{Ts}tacn)$] ($^{CO2Et}\mathbf{1}$, $E(Co^{II/I}) = -0.96$ V *vs.* SCE), the selectivity also improved by 14%. Then, we increased the $^{CO2Et}\mathbf{1}$ concentration with the idea to increase [Co–H] and thus the HAT product ($Sel_{16a/(43a+16a)} =$ 76%, Fig. S.45 and S.46†).

Finally, lowering the light intensity (1.7×10^{-4} mmol hν·s^{-1}), **16** was selectively reduced over **43** with 100% selectivity (Fig. 2d and Table S.19†). GC monitoring of the reactions showed that **16** was consumed and converted to **16a**, whereas **43** remained virtually intact and *vice versa* (Fig. 2c and d).

As a summary of this section, the observed selectivity agrees with the existence of two competitive mechanistic scenarios involving: (i) SET + HAT for substrates than can be directly reduced such as acetophenone, and (ii) HAT for substrates with low reduction potentials that cannot be directly reduced by one electron from the PC such as aromatic olefins.

Conclusions

We developed a dual cobalt–copper catalytic system capable of reducing aromatic olefins under simple operational conditions, solely using H_2O and an amine (Et_3N or $^{i}Pr_2EtN$) as the source of hydrides and visible light as the driving force. Our mechanistic studies based on reactivity and selectivity studies, catalyst design, deuterium-labelling and radical-clock experiments support a well-defined cobalt hydride as the intermediate responsible for the reductions, most likely through a HAT mechanism, discarding free radical diffusion as the main pathway. These results show that the selectivity of the metal hydrides in basic media can be controlled and directed to the reduction of organic functionalities. For this reason, we envision that other readily available H_2O reduction catalysts could also be active in the reduction of other functional groups and more complex organic structures. These results pave the way for the development of selective organic reductions and solar-chemical generation using artificial catalytic systems that operate entirely with earth-abundant elements, using visible light as the driving force and H_2O as a source of hydrides.

Data availability

All the data is provided in the ESI.†

Author contributions

AC identified the potential of olefin reduction at an early satge; CC performed most of the experiments as well as the DFT calculations, worked with AC and ICR on the synthesis of the photoredox catalysts, with AC on the optimisation studies, with DP and JA on the selectivity studies, wrote the manuscript together with JL and brought the project to completion. JL oversaw the project, discussed the results, and edited the manuscript. Moreover, all authors contributed with fruitful discussions to the manuscript.

Conflicts of interest

There are no conflicts to declare.

Acknowledgements

We would like to thank the European Commission for the ERC-CG-2014-648304 (J. Ll.-F.) project. The Spanish Ministry of Science is acknowledged for a FPU fellowship to C. C. (FPU14/02550) and A. C. and a Juan de la Cierva contract to A. C. The Spanish Ministry of Science is acknowledged for projects (PID2019-110050RB-I00 and CTQ2016-80038-R) and the MCIN/AEI/10.13039/501100011033 (CEX2019-000925-S). We also thank Catexel for a generous gift of tritosyl-1,4,7-triazacyclononane. The financial support from ICIQ Foundation and CELLEX Foundation through the CELLEX-ICIQ high throughput experimentation platform is acknowledged. We also thank CERCA Programme (Generalitat de Catalunya) for financial support. We thank Dr Ferran Acuña-Parés for fruitful discussions.

Notes and references

1 J. Barber and P. D. Tran, *J. R. Soc., Interface*, 2013, **10**, 20120984.
2 R. E. Galian and J. Pérez-Prieto, *Energy Environ. Sci.*, 2010, **3**, 1488.
3 C. R. Stephenson and T. P. Yoon, *Acc. Chem. Res.*, 2016, **49**, 2059–2060.
4 B. Zhang and L. Sun, *Chem. Soc. Rev.*, 2019, **48**, 2216–2264.
5 N. S. Lewis and D. G. Nocera, *Proc. Natl. Acad. Sci. U. S. A.*, 2006, **103**, 15729–15735.

6 T. R. Cook, D. K. Dogutan, S. Y. Reece, Y. Surendranath, T. S. Teets and D. G. Nocera, *Chem. Rev.*, 2010, **110**, 6474–6502.
7 E. S. Andreiadis, M. Chavarot-Kerlidou, M. Fontecave and V. Artero, *Photochem. Photobiol.*, 2011, **87**, 946–964.
8 K. E. Dalle, J. Warnan, J. J. Leung, B. Reuillard, I. S. Karmel and E. Reisner, *Chem. Rev.*, 2019, **119**, 2752–2875.
9 Z. Han and R. Eisenberg, *Acc. Chem. Res.*, 2014, **47**, 2537–2544.
10 V. S. Thoi, Y. Sun, J. R. Long and C. J. Chang, *Chem. Soc. Rev.*, 2013, **42**, 2388–2400.
11 D. Z. Zee, T. Chantarojsiri, J. R. Long and C. J. Chang, *Acc. Chem. Res.*, 2015, **48**, 2027–2036.
12 N. Kaeffer, M. Chavarot-Kerlidou and V. Artero, *Acc. Chem. Res.*, 2015, **48**, 1286–1295.
13 N. Queyriaux, R. T. Jane, J. Massin, V. Artero and M. Chavarot-Kerlidou, *Coord. Chem. Rev.*, 2015, **304–305**, 3–19.
14 A. M. Appel, J. E. Bercaw, A. B. Bocarsly, H. Dobbek, D. L. DuBois, M. Dupuis, J. G. Ferry, E. Fujita, R. Hille, P. J. Kenis, C. A. Kerfeld, R. H. Morris, C. H. Peden, A. R. Portis, S. W. Ragsdale, T. B. Rauchfuss, J. N. Reek, L. C. Seefeldt, R. K. Thauer and G. L. Waldrop, *Chem. Rev.*, 2013, **113**, 6621–6658.
15 J. Qiao, Y. Liu, F. Hong and J. Zhang, *Chem. Soc. Rev.*, 2014, **43**, 631–675.
16 C. Costentin, M. Robert and J. M. Saveant, *Chem. Soc. Rev.*, 2013, **42**, 2423–2436.
17 S. Boddu, S. T. Nishanthi and K. Kailasam, in *Visible Light-Active Photocatalysis*, 2018, pp. 421–446, DOI: 10.1002/9783527808175.ch15.
18 F. Franco, S. Fernández and J. Lloret-Fillol, *Curr. Opin. Electrochem.*, 2019, **15**, 109–117.
19 G. Palmisano, V. Augugliaro, M. Pagliaro and L. Palmisano, *Chem. Commun.*, 2007, 3425–3437, DOI: 10.1039/b700395c.
20 S. Choudhury, J. O. Baeg, N. J. Park and R. K. Yadav, *Angew. Chem., Int. Ed.*, 2012, **51**, 11624–11628.
21 S. H. Lee, J. H. Kim and C. B. Park, *Chem.–Eur. J.*, 2013, **19**, 4392–4406.
22 M. Mifsud, S. Gargiulo, S. Iborra, I. W. Arends, F. Hollmann and A. Corma, *Nat. Commun.*, 2014, **5**, 3145.
23 J. H. Kim, D. H. Nam and C. B. Park, *Curr. Opin. Biotechnol.*, 2014, **28**, 1–9.
24 J. Liu, J. Huang, H. Zhou and M. Antonietti, *ACS Appl. Mater. Interfaces*, 2014, **6**, 8434–8440.
25 A. Bachmeier, B. J. Murphy and F. A. Armstrong, *J. Am. Chem. Soc.*, 2014, **136**, 12876–12879.
26 E. S. Andreiadis, M. Chavarot-Kerlidou, M. Fontecave and V. Artero, *Photochem. Photobiol.*, 2011, **87**, 946–964.
27 J. A. Macia-Agullo, A. Corma and H. Garcia, *Chem.–Eur. J.*, 2015, **21**, 10940–10959.
28 P. De Luna, C. Hahn, D. Higgins, S. A. Jaffer, T. F. Jaramillo and E. H. Sargent, *Science*, 2019, **364**, eaav3506.
29 A. Call, C. Casadevall, F. Acuna-Pares, A. Casitas and J. Lloret-Fillol, *Chem. Sci.*, 2017, **8**, 4739–4749.
30 A. Call and J. Lloret-Fillol, *Chem. Commun.*, 2018, **54**, 9643–9646.
31 C. Casadevall, PhD thesis, Universitat Rovira i Virgili, 2019.
32 J. Lloret-Fillol, A. Casitas, A. Call and C. Casadevall, Photocatalytic Reduction Process and catalytic composition used in the process, Spain Patent, Submitted as: PCT. Fundació privada Institut Català d'Investigació Química, Application No PCT/ES2017/070314, application date 10.05.2017.
33 L. Alig, M. Fritz and S. Schneider, *Chem. Rev.*, 2019, **119**, 2681–2751.
34 M. Trincado, J. Bösken and H. Grützmacher, *Coord. Chem. Rev.*, 2021, **443**, 213967.
35 W. Ai, R. Zhong, X. Liu and Q. Liu, *Chem. Rev.*, 2019, **119**, 2876–2953.
36 J. Wen, F. Wang and X. Zhang, *Chem. Soc. Rev.*, 2021, **50**, 3211–3237.
37 L. Zhang, M. Zhou, A. Wang and T. Zhang, *Chem. Rev.*, 2020, **120**, 683–733.
38 A. J. Perkowski, W. You and D. A. Nicewicz, *J. Am. Chem. Soc.*, 2015, **137**, 7580–7583.
39 K. Imamura, Y. Okubo, T. Ito, A. Tanaka, K. Hashimoto and H. Kominami, *RSC Adv.*, 2014, **4**, 19883–19886.
40 J. Li, J. Yang, F. Wen and C. Li, *Chem. Commun.*, 2011, **47**, 7080–7082.
41 H. Yamataka, N. Seto, J. Ichihara, T. Hanafusa and S. Teratani, *J. Chem. Soc., Chem. Commun.*, 1985, 788–789, DOI: 10.1039/c39850000788.
42 H. Shimakoshi and Y. Hisaeda, *ChemPlusChem*, 2014, **79**, 1250–1253.
43 T. Shiragami, C. Pac and S. Yanagida, *J. Phys. Chem.*, 1990, **94**, 504–506.
44 Z. C. Litman, Y. Wang, H. Zhao and J. F. Hartwig, *Nature*, 2018, **560**, 355–359.
45 N. A. Larionova, J. M. Ondozabal and X. C. Cambeiro, *Adv. Synth. Catal.*, 2021, **363**, 558–564.
46 Y. Kamei, Y. Seino, Y. Yamaguchi, T. Yoshino, S. Maeda, M. Kojima and S. Matsunaga, *Nat. Commun.*, 2021, **12**, 966.
47 J. B. Metternich and R. Gilmour, *J. Am. Chem. Soc.*, 2015, **137**, 11254–11257.
48 J. Saltiel and G. S. Hammond, *J. Am. Chem. Soc.*, 1963, **85**, 2515–2516.
49 G. S. Hammond and J. Saltiel, *J. Am. Chem. Soc.*, 1962, **84**, 4983–4984.
50 M. R. Schreier, B. Pfund, X. Guo and O. S. Wenger, *Chem. Sci.*, 2020, **11**, 8582–8594.
51 M. L. Czyz, M. S. Taylor, T. H. Horngren and A. Polyzos, *ACS Catal.*, 2021, 5472–5480, DOI: 10.1021/acscatal.1c01000.
52 S. P. Luo, E. Mejia, A. Friedrich, A. Pazidis, H. Junge, A. E. Surkus, R. Jackstell, S. Denurra, S. Gladiali, S. Lochbrunner and M. Beller, *Angew. Chem., Int. Ed.*, 2013, **52**, 419–423.
53 A. Call, Z. Codolà, F. Acuña-Parés and J. Lloret-Fillol, *Chem.–Eur. J.*, 2014, **20**, 6171–6183.
54 J. Lloret-Fillol, C. Casadevall, J. León, A. Call, A. Casitas, J. J. Pla, P. J. Hernández and X. F. Caldentey, Photoreactor, Submitted as, *European Patent*, Fundació privada Institut Català d'Investigació Química, Application No 17382313.9-1370, application date 31.05.2017.

55 A. Call, F. Franco, N. Kandoth, S. Fernández, M. González-Béjar, J. Pérez-Prieto, J. M. Luis and J. Lloret-Fillol, *Chem. Sci.*, 2018, **9**, 2609–2619.
56 J. Lloret-Fillol, Z. Codolà, I. Garcia-Bosch, L. Gómez, J. J. Pla and M. Costas, *Nat. Chem.*, 2011, **3**, 807–813.
57 I. Ghosh, T. Ghosh, J. I. Bardagi and B. König, *Science*, 2014, **346**, 725–728.
58 The bond dissociation energy (BDE) is lower for aryl bromides than for other aryl halides (DFT calculated bond dissociation energies are as follows: BDE_{C-Br} = 81.9 kcal mol^{-1} for substrate **22**, BDE_{C-Cl} = 93.8 kcal mol^{-1} for **23**, and BDE_{C-F} = 126.0 kcal mol^{-1} for **25**).
59 E. S. Wiedner, M. B. Chambers, C. L. Pitman, R. M. Bullock, A. J. Miller and A. M. Appel, *Chem. Rev.*, 2016, **116**, 8655–8692.
60 Y. Hu, A. P. Shaw, D. P. Estes and J. R. Norton, *Chem. Rev.*, 2016, **116**, 8427–8462.
61 S. W. Crossley, C. Obradors, R. M. Martinez and R. A. Shenvi, *Chem. Rev.*, 2016, **116**, 8912–9000.
62 J. C. Lo, J. Gui, Y. Yabe, C. M. Pan and P. S. Baran, *Nature*, 2014, **516**, 343–348.
63 J. C. Lo, Y. Yabe and P. S. Baran, *J. Am. Chem. Soc.*, 2014, **136**, 1304–1307.
64 G. Li, A. Han, M. E. Pulling, D. P. Estes and J. R. Norton, *J. Am. Chem. Soc.*, 2012, **134**, 14662–14665.
65 D. C. Eisenberg and J. R. Norton, *Isr. J. Chem.*, 1991, **31**, 55.
66 S. Sang, T. Unruh, S. Demeshko, L. I. Domenianni, N. P. van Leest, P. Marquetand, F. Schneck, C. Würtele, F. J. de Zwart, B. de Bruin, L. González, P. Vöhringer and S. Schneider, *Chem.–Eur. J.*, 2021, **27**, 16978–16989.
67 G. Litwinienko and K. U. Ingold, *Acc. Chem. Res.*, 2007, **40**, 222–230.
68 H. Seo, M. H. Katcher and T. F. Jamison, *Nat. Chem.*, 2017, **9**, 453–456.
69 J.-W. Wang, K. Yamauchi, H.-H. Huang, J.-K. Sun, Z.-M. Luo, D.-C. Zhong, T.-B. Lu and K. Sakai, *Angew. Chem., Int. Ed.*, 2019, **58**, 10923–10927.
70 M. R. Friedfeld, H. Zhong, R. T. Ruck, M. Shevlin and P. J. Chirik, *Science*, 2018, **360**, 888–893.
71 M. R. Friedfeld, M. Shevlin, J. M. Hoyt, S. W. Krska, M. T. Tudge and P. J. Chirik, *Science*, 2013, **342**, 1076–1080.
72 W. Liu, B. Sahoo, K. Junge and M. Beller, *Acc. Chem. Res.*, 2018, **51**, 1858–1869.
73 J. P. Stevenson, W. F. Jackson and J. M. Tanko, *J. Am. Chem. Soc.*, 2002, **124**, 4271–4281.
74 R. Hollis, L. Hughes, V. W. Bowry and K. U. Ingold, *J. Org. Chem.*, 1992, **57**, 4284–4287.
75 J. Masnovi, E. G. Samsel and R. M. Bullock, *J. Chem. Soc., Chem. Commun.*, 1989, 1044–1045, DOI: 10.1039/C39890001044.
76 E. Mejía, S.-P. Luo, M. Karnahl, A. Friedrich, S. Tschierlei, A.-E. Surkus, H. Junge, S. Gladiali, S. Lochbrunner and M. Beller, *Chem.–Eur. J.*, 2013, **19**, 15972–15978.
77 S. Fischer, D. Hollmann, S. Tschierlei, M. Karnahl, N. Rockstroh, E. Barsch, P. Schwarzbach, S.-P. Luo, H. Junge, M. Beller, S. Lochbrunner, R. Ludwig and A. Brückner, *ACS Catal.*, 2014, **4**, 1845–1849.
78 S. Fernández, F. Franco, C. Casadevall, V. Martin-Diaconescu, J. M. Luis and J. Lloret-Fillol, *J. Am. Chem. Soc.*, 2020, **142**, 120–133.